Metabolic pathway analysis of an *Acinetobacter* strain capable of assimilating diverse hydrocarbons

Shori Inoue, Shogo Yoshimoto and Katsutoshi Hori[#]

Department of Biomolecular Engineering, Graduate School of Engineering, Nagoya University, Furo-cho, Chikusa-ku, Nagoya, Aichi 464-8603, Japan

Correspondence: Katsutoshi Hori

Department of Biomolecular Engineering, Graduate School of Engineering, Nagoya University, Furo-cho, Chikusa-ku, Nagoya, Aichi 464-8603, Japan.

Tel: +81-52-789-3339

Email: khori@chembio.nagoya-u.ac.jp

ABSTRACT

The growing demand for sustainable bioproduction requires the development of robust microbial chassis with broad metabolic versatility and suitability for industrial applications. *Acinetobacter* sp. Tol 5 is a highly adhesive bacterium capable of utilizing various hydrocarbons, making it a promising chassis for immobilized whole-cell catalysis. In this study, we characterized the carbon metabolism of Tol 5 by reconstructing metabolic pathway maps from its genomic data and analyzing the transcriptomes of cells grown on ethanol, hexadecane, toluene, phenol, and L-phenylalanine. Genomic analysis revealed that Tol 5 possesses a wide range of metabolic pathways for both alkanes and aromatics, including five distinct aromatic degradation routes. Transcriptome analysis identified the specific carbon sources that regulate each degradation pathway. Most pathways were induced by their corresponding carbon sources with high specificity, whereas some were upregulated by multiple related substrates. In addition, Tol 5 appears to metabolize phenylalanine via the homogentisate pathway, which differs from the phenylacetate pathway reported in *Acinetobacter baumannii*. Genes involved in oxidative and osmotic stress resistance were also coordinately upregulated on hydrocarbon sources, indicating adaptation to these cellular stresses associated with carbon sources. These results provide a comprehensive view of the carbon metabolism of Tol 5 and highlight its potential as a robust microbial chassis for converting non-sugar feedstocks into valuable bioproducts, while revealing new aspects of metabolic versatility in the genus *Acinetobacter*.

IMPORTANCE

Members of the genus *Acinetobacter* are ubiquitous environmental bacteria, which have attracted increasing attention in ecological and biotechnological fields due to their broad metabolic versatility and strong tolerance to environmental stress. We characterized the carbon metabolism of the hydrocarbon-degrading strain Tol 5 and identified five aromatic degradation pathways, including a toluene dioxygenase pathway and a homogentisate pathway, which are rarely reported in this genus. These findings expand the known metabolic repertoire of *Acinetobacter* and reveal that Tol 5 possesses aromatic degradation capabilities comparable to those of *Pseudomonas putida* strains, which are widely used as chassis for aromatic compound bioconversions. Furthermore, since aromatic compound metabolism has been reported to be associated with virulence and antibiotic resistance in pathogenic *Acinetobacter* strains, these insights may contribute to future strategies for pathogen control as well as leading the rational design of microbial chassis for sustainable bioproduction.

INTRODUCTION

In recent years, there has been a global shift from petrochemical synthesis to more sustainable bioprocesses, driven by the need to reduce fossil resource consumption and lessen environmental impact. Microorganisms, especially bacteria, are considered useful hosts for bioproduction due to their rapid growth, ease of genetic manipulation, and capacity for engineering to improve the productivity of valuable compounds. *Escherichia coli* is one of the most widely used microbial chassis in bioproduction, owing to its well-characterized molecular biology and metabolic systems (1). Concurrently, environmental microorganisms capable of assimilating non-sugar carbon substrates, such as C1 compounds, aromatic hydrocarbons, and oils, are increasingly valued for converting underutilized resources, including petrochemical by-products, agricultural waste, lignocellulosic biomass, and exhaust gases into valuable products (2-4). Therefore, it is essential to explore and develop new microbial chassis that can metabolize diverse substrates, tolerate environmental conditions, and perform robustly in industrial bioprocesses.

Members of the genus *Acinetobacter* are ubiquitous and found in diverse environments, including soil, oceans, freshwater, sediments, activated sludge, and clinical settings (5, 6). The genus possesses extensive genomic plasticity, which contributes to the pathogenic potential of some species. However, this trait, combined with a high tolerance to environmental stress, has also made it a focus of great interest in environmental microbiology, where several species have shown potential in bioproduction and bioremediation. For example, *A. baylyi* ADP1 has been studied as a host for the valorization of aromatic compounds via the β-ketoadipate pathway (5-7). *A. venetianus* RAG-1, which has multiple alkane hydroxylase genes, exhibits a pronounced ability to degrade crude oil and has been employed in bioremediation applications (8). Furthermore, *A. junii* BP25 has been utilized for the production of polyhydroxyalkanoates (PHAs) from food waste-derived organic acids, while *A. venetianus* AMO1502 has been applied in the biosynthesis of bioemulsifiers (9, 10).

Acinetobacter sp. Tol 5, originally isolated as a toluene-degrading bacterium from an exhaust gas treatment reactor, can degrade various hydrocarbons, including benzene, toluene, and xylene (BTX) (11). In addition to metabolic versatility, Tol 5 exhibits rapid autoagglutination and high adhesiveness to various solid materials, such as plastics, glass, and metals (12). This adhesive phenotype is mediated by its fibrous cell surface protein AtaA, a member of the trimeric autotransporter adhesin (TAA) family proteins (13). Previous studies have revealed the functional domains and biophysical properties of AtaA (14-16). Based on these findings, a reversible cell immobilization method was proposed to enhance the efficiency and productivity of bioproduction processes (17). To demonstrate its utility, Tol 5 expressing heterologous biosynthetic genes was immobilized on porous carriers and successfully utilized in an unconventional gas-phase bioreaction process to produce a high-value-added monoterpenoid (18). Although these advances indicate that Tol 5 is a promising microbial chassis for

85 innovative bioproduction, its central metabolic network remains largely uncharacterized.

86 In this study, we characterized the carbon metabolism of Tol 5 by reconstructing metabolic pathways
87 from the complete genome sequence and performing transcriptomic analyses of Tol 5 cells grown on
88 ethanol, hexadecane, or aromatic compounds as the sole carbon source. The results showed that Tol 5
89 metabolizes a variety of non-sugar carbon sources and regulates the corresponding metabolic
90 pathways in response to the carbon source.

91

92 **RESULTS**

93 **Central carbon metabolism**

94 The complete genome of Tol 5 consists of two circular DNA components, a chromosome of
95 4,681,789 bp and a plasmid of 117,717 bp, collectively encoding 4,404 predicted coding sequences
96 (CDSs) (19). We first evaluated the functional annotation of each CDS using multiple databases,
97 including NCBI, UniProtKB/Swiss-Prot, KEGG, and EggNOG, as well as information from relevant
98 literature (Table S1). Tol 5 encodes all the enzymes for gluconeogenesis, pentose phosphate pathway,
99 tricarboxylic acid (TCA) cycle, glyoxylate shunt, purine and pyrimidine biosynthesis, β-oxidation, and
100 fatty acid biosynthesis (Fig. 1, Table S2). In contrast, glycolysis via the Embden–Meyerhof–Parnas
101 (EMP) pathway is incomplete due to the absence of hexokinase, phosphofructokinase, and pyruvate
102 kinase, which is a trait commonly observed among *Acinetobacter* species (20). While some
103 *Acinetobacter* strains, such as *A. baylyi* ADP1 and *A. baumannii*, metabolize glucose via nonspecific
104 pyrroloquinoline quinone-dependent aldose dehydrogenase and the Entner–Doudoroff (ED) pathway
105 (21-23), Tol 5 completely lacks these genes. Furthermore, *A. baumannii* ATCC 19606 metabolizes
106 pentoses such as L-arabinose, D-xylose, and D-ribose via a pathway encoded by *ara* genes that
107 converts them into α-ketoglutarate (24), but Tol 5 also lacks the *ara* genes. These results suggest that
108 Tol 5 has a very limited capacity for sugar utilization as carbon sources.

109 Many *Acinetobacter* strains utilize organic acids and fatty acids as carbon sources (23). Tol 5 possesses
110 three acetate assimilation routes, including the reversible acetate kinase-phosphotransacetylase
111 (AckA-Pta) pathway, the irreversible acetyl-CoA synthetase (ACS) pathway, and the reversible
112 pathway mediated by succinyl-CoA:coenzyme A transferase AarC (Fig. 1, Table S2). For fatty acid
113 degradation, multiple candidate genes corresponding to each step of β-oxidation were identified,
114 including two putative acyl-CoA ligases, twelve acyl-CoA dehydrogenases, four enoyl-CoA
115 hydratases, and three thiolases. Propionyl-CoA generated during the β-oxidation of odd-chain fatty
116 acids was predicted to be catabolized to succinate and pyruvate via the methylcitrate cycle, which
117 consists of 2-methylisocitrate lyase (PrpB), 2-methylcitrate synthase (PrpC), 2-methylcitrate

118 dehydratase (AcnD), 2-methylaconitate isomerase (PrpF), bifunctional aconitate hydratase/isomerase
119 (AcnA and/or AcnB), and 2-methylisocitrate lyase (PrpB). In addition, four extracellular lipase genes
120 were identified in Tol 5 (Table S1), all of which are tandemly arranged (*TOL5_03740–TOL5_03770*)
121 and share 44–52% amino acid sequence identities with the triacylglycerol lipase Lip reported in *P.*
122 *aeruginosa* PAO1 (25). Tol 5 further encodes key enzymes that redirect fatty acid oxidation
123 intermediates into carbon storage compounds. A bifunctional wax ester synthase/acyl-
124 CoA:diacylglycerol acyltransferase (WS/DGAT, AtfA) mediates the production of wax esters and
125 triacylglycerols, while polyhydroxyalkanoate synthase (PhaC) is responsible for the production of
126 PHAs.

127

128 **Alkane metabolism**

129 Under aerobic conditions, *n*-alkanes are first oxidized at their terminal methyl group to primary
130 alcohols by alkane hydroxylases, and these alcohols are then further oxidized to aldehydes and finally
131 to fatty acids (26). The Tol 5 chromosome encodes multiple alkane hydroxylases, including a
132 membrane-bound non-heme iron alkane monooxygenase AlkB, and three flavin-containing
133 monooxygenases encoded by *almA*, *ladA_1*, *ladA_2* (Table S2). Additionally, the plasmid of Tol 5
134 carries a gene encoding an alkane hydroxylase (*TOL5_43480*), whose amino acid sequence shares
135 99% identity with that of a cytochrome P450 monooxygenase of the CYP153 family found in
136 *Acinetobacter* sp. EB104 (27). It also includes genes encoding associated redox partners, ferredoxin
137 (*TOL5_43490*) and ferredoxin reductase (*TOL5_43470*). AlkB and CYP153 typically oxidize short-
138 and medium-chain *n*-alkanes (C16 or less), whereas AlmA and LadA act on long-chain *n*-alkanes (C20
139 or more) (28-30). The presence of enzymes targeting various *n*-alkane chain lengths suggests that Tol
140 5 can efficiently degrade a wide range of alkanes. The resulting primary alcohols are further oxidized
141 by alcohol dehydrogenases (ADHs) and aldehyde dehydrogenases (ALDHs). In Tol 5 genome, at least
142 six putative ADH genes and one ALDH gene were predicted to be involved in fatty alcohol and fatty
143 aldehyde oxidation (Table S2). Although the functions of most ADHs in Tol 5 remain unclear, the iron-
144 containing ADH encoded by *yiaY_1* shares 91% amino acid sequence identity with ADH4 from *A.*
145 *baumannii* ATCC 19606, which catalyzes the oxidation of ethanol, 1-propanol, and 1-butanol (31).
146 The putative ALDH encoded by *aldB* (AldB) shares 87% amino acid identity with a long-chain ALDH,
147 Ald1, reported in *Acinetobacter* sp. M-1 (46).

148

149 **Aromatic compounds metabolism**

150 Genes encoding multi-component oxygenases for aromatic compound oxidation, as well as enzymes

151 for successive reaction steps leading to central metabolites, are generally organized into operons and
152 regulated by specific transcriptional regulators (32). Based on the predicted operons involved in
153 aromatic compound degradation (Table S2, Fig. 2), we reconstructed the aromatic degradation
154 pathways in Tol 5, identifying five major aromatic degradation routes, TOD, PCA, CAT, PAA, and
155 HMG pathways (Fig. 3).

156 The *pca* genes encode the enzymes responsible for the degradation of protocatechuate via the PCA
157 pathway (Fig. 3), forming a gene cluster together with the aromatic compounds transport protein PcaK
158 and the transcriptional repressor PcaU (Fig. 2). The *cat* gene cluster encodes the enzymes responsible
159 for the degradation of catechol via the CAT pathway (Fig. 3) and the transcriptional activator CatM.
160 Protocatechuate and catechol are common intermediates derived from various aromatic compounds
161 through various upstream pathways. The PCA and CAT pathways funnel these intermediates into
162 acetyl-CoA and succinyl-CoA, serving as central routes for aromatic compound degradation that are
163 widely conserved in *Acinetobacter* species (21, 33-35). In Tol 5, the *pca* genes are located adjacent to
164 the *qui* genes (Fig. 2), which encode enzymes that convert quinate and shikimate to protocatechuate
165 (Fig. 3). The structure of this gene cluster is similar to that reported in *A. baylyi* ADP1 (36), and as
166 described for ADP1, the *pca* and *qui* genes are likely organized as a large single operon under the
167 regulator PcaU in Tol 5. Tol 5 also possesses the *pob* and *van* genes, which encode upstream pathways
168 leading to protocatechuate, along with their respective transcriptional regulators (PobR and VanR)
169 (Fig. 2 and 3). The *cat* genes are located adjacent to the *mph* gene cluster, which encodes the
170 components of the phenol monooxygenase complex MphKLMNOP, catechol 1,2-dioxygenase CatA
171 (encoded by *catA_2*), and the regulatory proteins MphX (repressor) and MphR (activator) (Fig. 2).
172 The structure of the *mph* operon in Tol 5 resembles that of *A. calcoaceticus* PHEA-2 (37), but is
173 distinguished by the presence of the additional *catA* gene (*catA_2*) located immediately downstream
174 in the same operon. In addition, Tol 5 possesses the *ben* and *iac* genes, which encode enzymes for the
175 upstream pathways that lead to catechol, along with their respective transcriptional regulators (BenM
176 and IacR) and transporters (BenE, BenK, and a putative transporter encoded by *TOL5_19290*) (Fig. 2
177 and 3). Notably, the *ben* genes in Tol 5 are located over 900 kbp away from the *cat* operon, in contrast
178 to *A. baylyi* ADP1, in which the *ben* genes are located adjacent to the *cat* genes to facilitate coordinated
179 regulation of gene expression (38). Despite its distinct genomic location, the *ben* operon in Tol 5
180 includes the third *catA* gene (encoded by *catA_4*), indicating that coordinated regulation between the
181 *ben* and *cat* genes is maintained.

182 The *tod* operon encodes the enzymes of the toluene dioxygenase (TOD) pathway (Fig. 3) and is located
183 between the *todS*-*todT* two-component regulatory system and the putative toluene transporter gene
184 *fadL2*, which is located in a separate operon (Fig. 2). In the TOD pathway, toluene is oxidized into 3-
185 methylcatechol and ultimately converted into acetate, pyruvate, and acetyl-CoA. Although rarely

186 found in other *Acinetobacter* species, the *tod* genes of Tol 5 share high similarity with those of *P.*
187 *putida* strains and play a central role in the degradation of toluene and benzene, thereby expanding the
188 aromatic-degrading capacity of the genus (39).

189 Furthermore, Tol 5 possesses the *paa* genes, which encode the enzymes of the phenylacetic acid (PAA)
190 pathway (Fig. 3), as well as the transcriptional repressor PaaX (Fig. 2). The PAA pathway degrades
191 phenylacetate via epoxidation of CoA thioesters. This pathway in *A. baumannii* strains is thought to
192 be primarily associated with phenylalanine degradation (40, 41). In addition, Tol 5 also possesses a
193 gene cluster encoding a putative homogentisate pathway (HMG pathway in Fig. 3), which includes 4-
194 hydroxyphenylpyruvate dioxygenase (HPD), an IclR-type transcriptional repressor (IclR),
195 maleylacetoacetate isomerase (MaiA), fumarylacetoacetase (FahA), 3-oxoacid CoA-transferase
196 subunits A and B (ScoA and ScoB), and an aromatic amino acid transporter (AroP), as well as a
197 putative homogentisate dioxygenase encoded by *TOL5_11140* (Fig. 2). Although the protein product
198 of *TOL5_11140* was annotated as a glyoxalase (Table S1), it shares 22.7% amino acid identity with
199 homogentisate 1,2-dioxygenase HmgA (B7VA96) and 18.8% amino acid identity with
200 metapyrocatechase XylE (Q04385) from *P. putida*. The HMG pathway in Tol 5 is likely involved in
201 tyrosine metabolism. However, because canonical pathways converting phenylalanine to
202 phenylacetate or to tyrosine were not identified, the phenylalanine degradation route in Tol 5 could
203 not be determined from the genomic information.

204

205 **Substrate-dependent transcriptomic responses to lactate, ethanol, and hexadecane**

206 The expression of genes involved in carbon catabolism is tightly regulated based on available carbon
207 sources, particularly for the degradation pathways of hydrocarbons and aromatic compounds that are
208 not directly linked to central metabolism (42). Therefore, we analyzed the transcriptomic responses of
209 Tol 5 to different carbon sources using RNA-seq (Table S3). Transcriptomes were compared between
210 Tol 5 cells grown on lactate and those grown on other carbon sources; differentially expressed genes
211 were defined by the thresholds of $|\log_2$ fold change (FC) $| > 1$, $\log_2$ counts per million (CPM) > 3, and
212 false discovery rate (FDR) < 0.05 (Fig. 4A and 5A, Table S4).

213 In ethanol culture, 17 genes were significantly upregulated, including *yiaY_1* and *aldB*, which encode
214 an iron-containing ADH and a putative ALDH, respectively (Table S5). Since *yiaY_1* was the only
215 ADH gene induced by ethanol, it is likely the primary ADH responsible for ethanol oxidation in Tol 5
216 (Fig. 4B). Although AldB shares 87% amino acid identity with Ald1 from *Acinetobacter* sp. M-1,
217 which has been characterized as a long-chain ALDH that is inactive toward short-chain substrates such
218 as acetaldehyde (43), its induction during growth on ethanol suggests that AldB functions differently
219 from Ald1 and catalyzes acetaldehyde oxidation in Tol 5. While Tol 5 possesses both the AckA-Pta

220 pathway and the ACS pathway for converting acetate into acetyl-CoA (Fig. 1), only the *pta* gene in
221 the AckA-Pta pathway was upregulated during growth on ethanol (Fig. 4B). Additionally, *aceA*, which
222 encodes isocitrate lyase of the glyoxylate shunt that bypasses the decarboxylation steps of the TCA
223 cycle and conserves carbon flux for gluconeogenesis (Fig. 1), was upregulated. A similar regulatory
224 pattern was observed in *A. oleivorans* DR1, where the AckA-Pta pathway and *aceA* were upregulated
225 during growth on acetate compared to succinate (44), suggesting that Tol 5 employs a similar strategy
226 for assimilating acetate when growing on ethanol.

227 In hexadecane culture, 515 genes were significantly upregulated (Table S5). Among the multiple
228 alkane hydroxylase genes in Tol 5, *alkB* and the CYP153 gene were specifically induced, indicating
229 their involvement in the initial hydroxylation of hexadecane (Fig. 4C). The genes encoding an iron-
230 containing ADH encoded by *yiaY_3* and a putative coniferyl aldehyde dehydrogenase encoded by *calB*
231 were also upregulated, suggesting their roles in oxidation of hexadecanol to hexadecanal and
232 subsequently to hexadecanoic acid. The genes involved in every step of the β-oxidation pathway were
233 upregulated. Among the multiple predicted enzymes for each step, only *fadD4* (one of the two
234 predicted acyl-CoA ligase genes) and *fadE*, *ydiO_3*, and *ydiO_5* (three of the twelve predicted acyl-
235 CoA dehydrogenase genes) were specifically induced (Fig. 4C).

236 Sixteen genes were downregulated in both ethanol and hexadecane cultures compared to lactate culture,
237 implying that these genes are specifically upregulated during growth on lactate (Table S5 and S6).
238 Among them, the *lldP*, *lldR*, *lldD_1*, and *dld* genes (Fig. 1), which form an operon similar to the
239 *lldPRD* operon involved in lactate metabolism reported in *A. baumannii,* were identified (45). The
240 *aceE* and *aceF* genes, which encode components of pyruvate dehydrogenase, were also upregulated
241 during growth on lactate. The *pca* and *qui* genes, responsible for quinate and shikimate utilization,
242 were downregulated in ethanol and hexadecane cultures, indicating catabolite repression similar to
243 that reported for *A. baylyi* ADP1, where these genes are repressed in the presence of preferred carbon
244 sources (33, 38).

245

246 **Substrate-specific regulation of aromatics degradation pathways**

247 The transcriptomes of Tol 5 cells grown on toluene, phenol, or L-phenylalanine were also compared
248 with those grown on lactate (Fig. 5A, Table S4). On these three carbon sources (toluene, phenol, and
249 L-phenylalanine), genes of the PCA pathway were downregulated, whereas the genes for other
250 aromatic compounds degradation pathways were upregulated, with each pathway most strongly
251 induced by its corresponding substrate (Fig. 5B and C, Table S5). In toluene culture, the TOD pathway
252 genes showed the highest induction among those of aromatic compounds degradation pathways (Fig.
253 5B). The *fadL2*, which is located adjacent to the *tod* operon and encodes a putative toluene transporter,

254 was also upregulated, although it was reported that its deletion did not affect growth on toluene (39).
255 In phenol culture, the *mph* genes and the CAT pathway genes were highly upregulated (Fig. 5B and
256 C). Additionally, the TOD pathway genes were significantly upregulated in phenol culture, with
257 expression levels of the genes comparable to those observed in toluene culture (Fig. 5B).

258 For L-phenylalanine, two degradation pathways, the PAA pathway and the HMG pathway, were
259 predicted in Tol 5 (Fig. 3). The transcriptome data showed that the upregulation of the HMG pathway
260 genes was marked in L-phenylalanine culture (Fig. 5B). Additionally, the *aco* operon, which encodes
261 enzymes for acetoacetate assimilation via acetoin, was upregulated, supporting the involvement of the
262 HMG pathway in phenylalanine metabolism, in which acetoacetate is generated as one of the final
263 metabolites (Fig. 5D and 5E, Table S5).

264 Aromatic substrates also influenced downstream central metabolic pathways (Fig. S1, Table S5).
265 Growth on these compounds triggered a differential response in aconitate hydratase isozymes, with
266 *acnA_2 b*eing upregulated, whereas *acnB* was downregulated. Concurrently, *pckG,* encoding the key
267 gluconeogenic enzyme phosphoenolpyruvate carboxykinase (46), was downregulated in all three
268 conditions, indicating a reduced carbon flux from the TCA cycle into gluconeogenesis.

269

270 **Expression of intracellular stress resistance genes under different carbon sources**

271 In addition to carbon metabolic pathways, genes involved in environmental stress resistance showed
272 significant transcriptional changes depending on the carbon sources (Fig. 6, Table S5). Notably,
273 several genes related to oxidative stress resistance were upregulated in Tol 5 cells grown on
274 hexadecane, toluene, phenol, or L-phenylalanine. The genes encoding monofunctional heme catalases
275 (*katA* and/or *katE*) were highly upregulated under all four conditions. The Mn/Fe superoxide
276 dismutase genes (*sodA_1* and/or *sodA_2*) were repressed in hexadecane and L-phenylalanine cultures
277 but upregulated in toluene and phenol cultures. The periplasmic Cu/Zn superoxide dismutase gene
278 (*sodC*) was upregulated in toluene, phenol, and L-phenylalanine cultures. The alkyl hydroperoxide
279 reductase genes (*ahpC_1* and *ahpC_2*), which play a role in peroxide detoxification, and the
280 methionine-(*S*)-sulfoxide reductase and methionine-(*R*)-sulfoxide reductase genes (*msrA* and *msrB*),
281 which repair oxidized methionine residues, were highly upregulated in L-phenylalanine culture.
282 Concurrently, the trehalose synthesis genes (*otsA* and *otsB*), associated with osmotic stress resistance
283 (47, 48), were also upregulated on all four alkane and aromatic carbon sources. The *otsB* gene, which
284 encodes trehalose-6-phosphate phosphatase, exhibited low expression levels ($\log_2$ CPM) but showed
285 high upregulation ($\log_2$ FC). These results indicate that Tol 5 activates mechanisms for oxidative and
286 osmotic stress resistance during growth on alkanes and aromatic compounds.

287

288 **DISCUSSION**

289 Members of the genus *Acinetobacter* inhabit diverse environments, including soil, oceans,
290 freshwater, sediments, activated sludge, and polluted sites (20, 49). Several *Acinetobacter* strains,
291 such as the *A. calcoaceticus–A. baumannii* complex, are also opportunistic nosocomial pathogens
292 that exhibit multidrug resistance (50). Consequently, most previous research on *Acinetobacter*
293 species has focused on antibiotic resistance, genomic plasticity, horizontal gene transfer, and
294 pathogenicity, whereas the metabolic capabilities of this genus remain comparatively underexplored
295 (20, 49). Although *A. baylyi* ADP1 is a widely used model strain and its 3.5 Mb genome has been
296 well characterized (21, 51), this genome is smaller than those of many other *Acinetobacter* species,
297 and thus represents only a subset of the metabolic potential present across the genus (20, 21). In this
298 study, we characterized the carbon metabolism of the highly adhesive hydrocarbon-degrading
299 *Acinetobacter* strain Tol 5, which has a 4.8 Mb genome (19). Genome and transcriptome analyses
300 revealed that Tol 5 has limited capability to metabolize sugars but possesses an extensive repertoire
301 of genes for alkane and aromatic metabolism and regulates them in response to available carbon
302 sources. In particular, this study identified the presence of the TOD and HMG pathways in
303 *Acinetobacter* species and demonstrated that the genes involved in these pathways are specifically
304 induced during growth on toluene and L-phenylalanine, respectively. Tol 5 also harbors the PAA
305 pathway, which in *A. baumannii* is primarily associated with phenylalanine degradation but was
306 weakly induced by L-phenylalanine in Tol 5. Because the PAA pathway has been implicated in the
307 degradation of other aromatics in *P. putida*, including phenylethylamine, phenylethanol, styrene, and
308 *n*-phenylalkanoates (52), it may also contribute to the degradation of multiple aromatic substrates in
309 Tol 5. These findings demonstrate that Tol 5 possesses a unique repertoire of aromatic degradation
310 pathways, combining routes broadly conserved in the genus *Acinetobacter* with additional pathways
311 (such as TOD and HMG) that are rare in this genus. This metabolic versatility is comparable to that
312 of *Pseudomonas putida* strains, widely used chassis for aromatic compound bioconversion. During
313 growth on hydrophobic carbon sources, such as hexadecane and aromatic compounds, oxidative and
314 osmotic stress resistance genes were also upregulated in Tol 5, indicating that these substrates
315 impose cellular stress and that Tol 5 expresses the corresponding stress response. These findings
316 provide new insights into the metabolic diversity of *Acinetobacter* species and demonstrate that Tol
317 5 can serve as a model with metabolic pathways distinct from those of previously well-characterized
318 species.

319 *Acinetobacter* species widely exhibit the capacity for alkane degradation, as more than 95% of
320 strains encode the alkane monooxygenases AlkB and AlmA (20). Oil-degrading strains such as *A.*
321 *venetianus* RAG-1 and *A. oleivorans* DR1 possess multiple AlkB homologs, enabling efficient

322 utilization of *n*-alkanes (8, 53). Although Tol 5 possesses only one *alkB* gene on the genome, it also
323 carries a plasmid-encoded cytochrome P450 monooxygenase of the CYP153 family. CYP153, which
324 is a distinct alkane hydroxylase targeting short- and medium-chain *n*-alkanes, is typically found in
325 alkane-degrading bacteria lacking AlkB but is relatively rare among *Acinetobacter* genomes (28, 54).
326 Both *alkB* and the CYP153 gene were induced in Tol 5 grown on hexadecane, indicating that Tol 5
327 employs both types of alkane hydroxylases to oxidize hexadecane efficiently (Fig. 4C and Table S5).

328 The expression of aromatic compound degradation pathways is generally regulated by pathway-
329 specific transcriptional regulators to prevent unnecessary synthesis of corresponding enzymes and
330 accumulation of toxic intermediates (55). In the TOD pathway, genes encoding all reaction steps for
331 toluene degradation, from the initial oxidation catalyzed by toluene dioxygenase to the generation of
332 pyruvate and acetyl-CoA, are clustered in a single *tod* operon (Fig. 2). This operon is regulated by
333 the TodS-TodT two-component system, in which the TodS senses a broad spectrum of aromatic
334 effectors, autophosphorylates, and activates transcription of the *tod* operon through phosphate
335 transfer to the transcriptional activator TodT (56, 57). Transcriptome analysis in Tol 5 revealed
336 distinct responses to different substrates: growth on phenol induced not only the *cat* and *mph* genes
337 (the latter including genes encoding phenol monooxygenase components) but also the *tod* genes,
338 whereas growth on toluene strongly induced only the *tod* operon (Fig. 5BC). Previous studies have
339 demonstrated that the toluene dioxygenase complex TodABC1C2, encoded by the *tod* operon,
340 oxidizes phenol to catechol and hydroquinone, and that a mutant of *P. putida* F1 lacking this enzyme
341 cannot grow on phenol as a sole carbon source (58, 59). Taken together, these findings suggest that
342 Tol 5 uses both toluene dioxygenase and phenol monooxygenase for phenol degradation.

343 The *cat* operon in Tol 5, which encodes the CAT pathway responsible for catechol degradation,
344 includes a catechol 1,2-dioxygenase gene *catA* (*catA_3*). Notably, homologs of the *catA* gene are
345 also present in both the *mph* and *ben* operons (Fig. 2). The presence of *catA* within the *mph* operon is
346 distinct from that in *A. calcoaceticus* PHEA-2 previously reported (37). Transcriptome analysis
347 revealed that this *catA* gene (*catA_2*) was induced with other *mph* genes at similar expression levels
348 by phenol (Fig. 5C), indicating that it is transcriptionally regulated as part of the same operon (Fig.
349 2). This genetic organization is analogous to the *ben* genes described in *P. putida* strains and *A.*
350 *baylyi* ADP1, where CatA encoded by the *ben* operon converts the catechol generated by benzoate
351 oxidation into *cis*,*cis*-muconate, and the *cis*,*cis*-muconate activates the downstream *cat* operon (60-
352 62). Such coordinated regulation prevents the accumulation of catechol, which is toxic at high
353 concentrations (63). Therefore, the organization of the *mph* operon as well as the *ben* operon in Tol 5
354 likely enables fine-tuned transcription during the degradation of phenol and probably benzoate,
355 representing an optimized gene organization for the degradation of aromatic compounds.

356 Carbon catabolic pathways are often subject to carbon catabolite repression (CCR) (42). In *A. baylyi*
357 ADP1, the catabolite repression control protein (Crc) represses the *pca* and *cat* operons (33, 38).
358 Succinate and acetate induce strong repression, whereas pyruvate and lactate cause relatively weak
359 repression. Tol 5 encodes a Crc homologue (TOL5_01610) that shares 89% amino acid identity with
360 ADP1 Crc, and both the *pca* and *cat* genes were repressed in Tol 5 during growth on ethanol, where
361 acetate is expected to accumulate (Fig. 5B, Table S5). This indicates that Tol 5 exhibits a similar
362 CCR. In addition, the *tod*, *paa*, and *hmg* genes showed a similar expression pattern, with lower
363 expression in lactate and ethanol cultures and higher expression under other carbon sources (Fig.
364 5B). This pattern may reflect CCR-like regulation that prioritizes the utilization of readily
365 metabolizable carbon sources, such as lactate and ethanol, over hydrocarbon degradation. Given that
366 disruption of CCR has been reported to markedly alter the utilization of aromatic substrates (64),
367 modulation of CCR should be considered a key strategy to control the expression of aromatic
368 compound metabolic pathways in Tol 5 for bioproduction applications.

369 Alkane and aromatic oxygenases catalyze the initial oxidation of their substrates by forming transient
370 radicals at the active site, which can lead to the leakage of reactive oxygen species (ROS) (65).
371 Consequently, ROS are considered to be by-products of alkane and aromatic hydroxylation, and cells
372 must deploy protective mechanisms to scavenge them. For instance, *A. calcoaceticus* grown on
373 hydrocarbons exhibits increased superoxide dismutase activity, while both *A. oleivorans* DR1 cultured
374 on triacontane and *Paraburkholderia xenovorans* p2-fldX1 grown on 4-hydroxyphenylacetate
375 upregulate multiple ROS scavengers (53, 65, 66). In Tol 5 grown on hexadecane or aromatic
376 compounds, oxidative stress resistance genes, including *sodA_2*, *sodC*, *katA*, *katE*, *msrA*, and *msrB*,
377 were similarly induced (Fig. 6). Furthermore, the expression of TCA cycle enzymes is also likely to
378 be replaced according to the intercellular oxidative stress. In *E. coli*, ROS-sensitive aconitate hydratase
379 AcnB functions as the primary aconitate hydratase during the growth phase, while ROS-tolerant
380 isozyme AcnA is induced under oxidative stress conditions to maintain the TCA cycle (67, 68). Thus,
381 the expression shift from *acnB* to *acnA_2* in the TCA cycle of Tol 5 grown on aromatic compounds
382 suggests that Tol 5 also replaces metabolic enzymes to maintain central metabolism in response to
383 intracellular oxidative stress (Fig. S1). In summary, Tol 5 responds to oxidative stress according to the
384 available carbon source, not only by activating stress resistance genes but also by replacing vulnerable
385 metabolic enzymes to sustain central metabolism under cellular stress.

386 In conclusion, Tol 5 possesses a diverse set of metabolic pathways for alkanes and aromatic
387 compounds, regulates these pathways according to available carbon sources, and activates stress
388 resistance genes. Owing to its strong adhesiveness and ability to metabolize alkanes and aromatic
389 compounds, Tol 5 represents a promising microbial chassis for bioprocesses utilizing non-sugar
390 substrates.

391

392 **MATERIALS AND METHODS**

393 **Genome sequence data analysis**

394 The complete genome sequence of Tol 5, consisting of a chromosome and a plasmid, was obtained
395 from the NCBI database (accession: AP024708 and AP024709). All amino acid sequences of the CDSs
396 were searched against the UniProtKB/Swiss-Prot database (as of August 2024) using BLASTP, and
397 the best-scoring hit for each CDS was used for functional annotation. The sequences were further
398 searched against the KEGG database using BlastKOALA and KEGG automatic annotation server
399 (accession: T11084). For CDSs, that could not be annotated with the KEGG database, additional
400 searches were performed against the EggNOG database using eggNOG-mapper. Based on the
401 annotations obtained, a central carbon metabolic pathway map was reconstructed using KEGG mapper.
402 Peripheral metabolic pathways, including those involved in the degradation of alkanes and aromatic
403 compounds, were inferred by comparing operon organization with those previously characterized in
404 closely related bacterial species. Operon structures were predicted using two tools: Operon-mapper
405 (69), which infers operons based on intergenic distances and gene functions, and Rockhopper (70),
406 which additionally incorporates transcriptomic data. Functional annotations, operon predictions, and
407 metabolic pathways were manually curated based on information from relevant literature.

408

409 **Growth conditions**

410 *Acinetobacter* sp. Tol 5 was cultured in 20 mL of basal salt (BS) medium (11) supplemented with a
411 single carbon source in 100-mL Erlenmeyer flasks. Each of DL-lactate, ethanol, hexadecane, toluene,
412 phenol, and L-phenylalanine was supplied as the sole carbon source at a carbon equivalent
413 concentration of 3.3×10^{-2} mol/L. Precultures were prepared by growing Tol 5 in lysogeny broth (LB)
414 medium supplemented with the corresponding carbon source. The pre-culture was washed twice with
415 an equal volume of BS medium and then inoculated into 20 mL of culture medium at a 1:100 ratio.
416 Four rectangular pieces of polyurethane foam support (10 × 10 × 10 mm, CFH-20, 20 pores/25 mm;
417 Inoac Corporation, Nagoya, Japan) were placed in each flask. The flasks were then capped with
418 silicone stoppers for lactate, ethanol, and L-phenylalanine, or with Viton rubber stoppers for
419 hexadecane, toluene, and phenol, and incubated at 28 °C with shaking at 115 rpm.

420

421 **RNA sequencing**

Tol 5 cells during growth were harvested by centrifugation (8,000 × g, 4°C, 3 min), and the cell pellets were stored at -30°C. For each growth condition, three biological replicates were prepared. Total RNA was extracted using the RNA Prep Kit (Cica Genus, Tokyo, Japan) according to the manufacturer's protocol. Ribosomal RNA was removed using the NEBNext rRNA Depletion Kit (Bacteria) (New England Biolabs, Ipswich, MA, USA), and cDNA libraries were generated with the NEBNext Ultra II RNA Library Prep Kit for Illumina (New England Biolabs, Ipswich, MA, USA). The cDNA libraries were sequenced on the Illumina NextSeq550. Raw FASTQ reads were quality-filtered using fastp (version 0.23.2) and mapped to the Tol 5 genome (accession: AP024708 and AP024709) using Bowtie2 (version 2.5.1) with default parameters. Mapped reads were counted using featureCounts (version 2.0.6).

Differential gene-expression analysis

Raw read counts of CDSs were analyzed in R using the edgeR package (version 3.42.4). Genes with extremely low expression were removed using the filterByExpr function. Normalization was performed using the trimmed mean of M-values (TMM) method implemented in the calcNormFactors function. Differential gene-expression analysis was conducted using the quasi-likelihood pipeline. A design matrix was constructed incorporating the cells grown on six different carbon sources (n = 3), with the data from those grown on lactate set as the reference group. Dispersion estimates were obtained using the estimateDisp function, and model fitting was performed with the glmQLFit function. Differential expression between each condition and the control condition (lactate condition) was assessed using the glmQLFTest function. Genes with FDR < 0.05, $\log_2$ FC > 1, and $\log_2$ CPM > 3 were extracted as significantly differentially expressed genes.

ACKNOWLEDGMENTS

The authors wish to acknowledge the Center for Gene Research, Nagoya University, for technical support with the RNA sequencing. The authors also thank Yuki Ohara for kindly discussing genome sequence data analysis and reviewing the manuscript.

This research was supported by the Graduate Program of Transformative Chem-Bio Research at Nagoya University supported by MEXT (WISE Program) to SI, the Japan Science and Technology Agency (JST) SPRING (Grant Number 8 JPMJSP2125) to SI, the Japan Society for the Promotion of Science (JSPS) KAKENHI (Grant Number JP24H00043) to KH and SY, and the GteX Program Japan Grant number JPMJGX23B4 to KH.

AUTHOR CONTRIBUTIONS

Shori Inoue: Conceptualization, Formal analysis, Investigation, Data curation, Writing - Original Draft. **Shogo Yoshimoto:** Conceptualization, Writing - Review & Editing. **Katsutoshi Hori:** Conceptualization, Supervision, Project administration, Writing - Review & Editing.

DATA AVAILABILITY

RNA-seq data reported are available in the DDBJ Sequenced Read Archive under the accession numbers PRJDB35996.

REFERENCE

1. Pontrelli S, Chiu T-Y, Lan EI, Chen FYH, Chang P, Liao JC. 2018. *Escherichia coli* as a host for metabolic engineering. *Metabolic Engineering* 50:16-46.

2. Liew FE, Nogle R, Abdalla T, Rasor BJ, Canter C, Jensen RO, Wang L, Strutz J, Chirania P, De Tissera S, Mueller AP, Ruan Z, Gao A, Tran L, Engle NL, Bromley JC, Daniell J, Conrado R, Tschaplinski TJ, Giannone RJ, Hettich RL, Karim AS, Simpson SD, Brown SD, Leang C, Jewett MC, Köpke M. 2022. Carbon-negative production of acetone and isopropanol by gas fermentation at industrial pilot scale. *Nature Biotechnology* 40:335-344.

3. Liu H, Tao X, Ntakirutimana S, Liu Z-H, Li BZ, Yuan YJ. 2024. Engineering *Pseudomonas putida* for lignin bioconversion into *cis-cis* muconic acid. *Chemical Engineering Journal* 495:153375.

4. Martín-González J, Montero-Bullón J-F, Muñoz-Fernández G, Buey RM, Jiménez A. 2025. Valorization of waste cooking oil for bioproduction of industrially-relevant metabolites in *Ashbya gossypii*. *New Biotechnology* 88:32-38.

5. Biggs BW, Bedore SR, Arvay E, Huang S, Subramanian H, McIntyre EA, Duscent-Maitland CV, Neidle EL, Tyo Keith E J. 2020. Development of a genetic toolset for the highly engineerable and metabolically versatile *Acinetobacter baylyi* ADP1. *Nucleic Acids Research* 48:5169-5182.

6. Luo J, McIntyre Emily A, Bedore Stacy R, Santala V, Neidle Ellen L, Santala S. 2022. Characterization of highly ferulate-tolerant *Acinetobacter baylyi* ADP1 isolates by a rapid reverse engineering method. *Applied and Environmental Microbiology* 88:e01780-21.

484 7. Kurnia K, Efimova E, Santala V, Santala S. 2024. Metabolic engineering of *Acinetobacter baylyi*
485 ADP1 for naringenin production. *Metabolic Engineering Communications* 19:e00249.

486 8. Liu J, Zhao B, Lan Y, Ma T. 2021. Enhanced degradation of different crude oils by defined
487 engineered consortia of *Acinetobacter venetianus* RAG-1 mutants based on their alkane
488 metabolism. *Bioresource Technology* 327:124787.

489 9. Sabapathy PC, Devaraj S, Parthipan A, Kathirvel P. 2019. Polyhydroxyalkanoate production
490 from statistically optimized media using rice mill effluent as sustainable substrate with an
491 analysis on the biopolymer's degradation potential. *International Journal of Biological*
492 *Macromolecules* 126:977-986.

493 10. D'Almeida AP, de Azevedo DCS, Melo VMM, de Albuquerque TL, Rocha MVP. 2024.
494 Bioemulsifier production by *Acinetobacter venetianus* AMO1502: Potential for bioremediation
495 and environmentally friendly applications. *Marine Pollution Bulletin* 203:116436.

496 11. Hori K, Yamashita S, Ishii Si, Kitagawa M, Tanji Y, Unno H. 2001. Isolation, Characterization
497 and application to off-gas treatment of toluene-degrading bacteria. *Journal of Chemical*
498 *Engineering of Japan* 34:1120-1126.

499 12. Ishikawa M, Shigemori K, Suzuki A, Hori K. 2012. Evaluation of adhesiveness of *Acinetobacter*
500 sp. Tol 5 to abiotic surfaces. *Journal of Bioscience and Bioengineering* 113:719-725.

501 13. Ishikawa M, Nakatani H, Hori K. 2012. AtaA, a new member of the trimeric autotransporter
502 adhesins from *Acinetobacter* sp. Tol 5 mediating high adhesiveness to various abiotic surfaces.
503 *PLOS ONE* 7:e48830.

504 14. Yoshimoto S, Aoki S, Ohara Y, Ishikawa M, Suzuki A, Linke D, Lupas AN, Hori K. 2023.
505 Identification of the adhesive domain of AtaA from *Acinetobacter* sp. Tol 5 and its application in
506 immobilizing *Escherichia coli*. *Frontiers in Bioengineering and Biotechnology* 10:1095057.

507 15. Yoshimoto S, Ishii S, Kawashiri A, Matsushita T, Linke D, Göttig S, Kempf VAJ, Takai M, Hori
508 K. 2024. Adhesion preference of the sticky bacterium *Acinetobacter* sp. Tol 5. *Frontiers in*
509 *Bioengineering and Biotechnology* 12:1342418.

510 16. Inoue S, Yoshimoto S, Hori K. 2025. A new target of multiple lysine methylation in bacteria.
511 *Journal of Bacteriology* 207:e00325-24.

512 17. Yoshimoto S, Ohara Y, Nakatani H, Hori K. 2017. Reversible bacterial immobilization based on
513 the salt-dependent adhesion of the bacterionanofiber protein AtaA. *Microbial Cell Factories*
514 16:123.

515 18. Usami A, Ishikawa M, Hori K. 2020. Gas-phase bioproduction of a high-value-added
516 monoterpenoid (*E*)-geranic acid by metabolically engineered *Acinetobacter* sp. Tol 5. *Green*
517 *Chemistry* 22:1258-1268.

518 19. Ishikawa M, Hori K. 2021. Complete genome sequence of the highly adhesive bacterium
519 *Acinetobacter* sp. strain Tol 5. *Microbiology Resource Announcements* 10:10.1128/mra.00567-
520 21.

521 20. Zhao Y, Wei HM, Yuan JL, Xu L, Sun JQ. 2023. A comprehensive genomic analysis provides
522 insights on the high environmental adaptability of *Acinetobacter* strains. *Frontiers in*
523 *Microbiology* 14:1177951.

524 21. Barbe V, Vallenet D, Fonknechten N, Kreimeyer A, Oztas S, Labarre L, Cruveiller S, Robert C,
525 Duprat S, Wincker P, Ornston LN, Weissenbach J, Marlière P, Cohen GN, Médigue C. 2004.
526 Unique features revealed by the genome sequence of *Acinetobacter* sp. ADP1, a versatile and
527 naturally transformation competent bacterium. *Nucleic Acids Research* 32:5766-5779.

528 22. Kannisto MS, Mangayil RK, Shrivastava-Bhattacharya A, Pletschke BI, Karp MT, Santala VP.
529 2015. Metabolic engineering of *Acinetobacter baylyi* ADP1 for removal of *Clostridium*
530 *butyricum* growth inhibitors produced from lignocellulosic hydrolysates. *Biotechnology for*
531 *Biofuels* 8:198.

532 23. Ren X, Palmer Lauren D. 2023. *Acinetobacter* metabolism in infection and antimicrobial
533 resistance. *Infection and Immunity* 91:e00433-22.

534 24. Alberti L, König P, Zeidler S, Poehlein A, Daniel R, Averhoff B, Müller V. 2023. Identification
535 and characterization of a novel pathway for aldopentose degradation in *Acinetobacter*
536 *baumannii*. *Environmental Microbiology* 25:2416-2430.

537 25. Wohlfarth S, Hoesche C, Strunk C, Winkler UK. 1992. Molecular genetics of the extracellular
538 lipase of *Pseudomonas aeruginosa* PAO1. *Microbiology* 138:1325-1335.

539 26. Rojo F. 2009. Degradation of alkanes by bacteria. *Environmental Microbiology* 11:2477-2490.

540 27. Maier T, Förster HH, Asperger O, Hahn U. 2001. Molecular characterization of the 56-kDa
541 CYP153 from *Acinetobacter* sp. EB104. *Biochemical and Biophysical Research*
542 *Communications* 286:652-658.

543 28. Nie Y, Chi CQ, Fang H, Liang JL, Lu SL, Lai GL, Tang YQ, Wu XL. 2014. Diverse alkane
544 hydroxylase genes in microorganisms and environments. *Scientific Reports* 4:4968.

545 29. Kong W, Zhao C, Gao X, Wang L, Tian Q, Liu Y, Xue S, Han Z, Chen F, Wang S. 2021.

546 Characterization and transcriptome analysis of a long-chain *n*-alkane-degrading strain
547 *Acinetobacter pittii* SW-1. *International Journal of Environmental Research and Public Health.*
548 18(12):6365.

549 30. Chen S, Cao L, Lv T, Liu J, Gao G, Li M, Sun L, Tian W, Tian Y, Li G, Ma T. 2024. Regulation
550 mechanism of the long-chain *n*-alkane monooxygenase gene *almA* in *Acinetobacter venetianus*
551 RAG-1. *Applied and Environmental Microbiology* 91:e02050-24.

552 31. Lin GH, Hsieh MC, Shu HY. 2021. Role of iron-containing alcohol dehydrogenases in
553 *Acinetobacter baumannii* ATCC 19606 stress resistance and virulence. *International Journal of*
554 *Molecular Sciences* 22(18):9921.

555 32. Phale PS, Malhotra H, Shah BA. 2020. Chapter One - Degradation strategies and associated
556 regulatory mechanisms/features for aromatic compound metabolism in bacteria, p 1-65. *In* Gadd
557 GM, Sariaslani S (ed), *Advances in Applied Microbiology*, vol 112. Academic Press.

558 33. Fischer R, Bleichrodt FS, Gerischer UC. 2008. Aromatic degradative pathways in *Acinetobacter*
559 *baylyi* underlie carbon catabolite repression. *Microbiology* 154:3095-3103.

560 34. Stuani L, Lechaplais C, Salminen AV, Ségurens B, Durot M, Castelli V, Pinet A, Labadie K,
561 Cruveiller S, Weissenbach J, de Berardinis V, Salanoubat M, Perret A. 2014. Novel metabolic
562 features in *Acinetobacter baylyi* ADP1 revealed by a multiomics approach. *Metabolomics*
563 10:1223-1238.

564 35. Breisch J, Huber LS, Kraiczy P, Hubloher J, Averhoff B. 2022. The ß-ketoadipate pathway of
565 *Acinetobacter baumannii* is involved in complement resistance and affects resistance against
566 aromatic antibiotics. *Environmental Microbiology Reports* 14:170-178.

567 36. Dal S, Trautwein G, Gerischer U. 2005. Transcriptional organization of genes for
568 protocatechuate and quinate degradation from *Acinetobacter* sp. strain ADP1. *Applied and*
569 *Environmental Microbiology* 71:1025-1034.

570 37. Yu H, Peng Z, Zhan Y, Wang J, Yan Y, Chen M, Lu W, Ping S, Zhang W, Zhao Z, Li S, Takeo M,
571 Lin M. 2011. Novel regulator MphX represses activation of phenol hydroxylase genes caused by
572 a XylR/DmpR-type regulator MphR in *Acinetobacter calcoaceticus*. *PLOS ONE* 6:e17350.

573 38. Bleichrodt FS, Fischer R, Gerischer UC. 2010. The β-ketoadipate pathway of *Acinetobacter*
574 *baylyi* undergoes carbon catabolite repression, cross-regulation and vertical regulation, and is
575 affected by Crc. *Microbiology* 156:1313-1322.

576 39. Yoshimoto S, Hattori M, Inoue S, Mori S, Ohara Y, Hori K. 2025. Identification of toluene

degradation genes in *Acinetobacter* sp. Tol 5. *Journal of Bioscience and Bioengineering* 140:284-289.

40. Hooppaw Anna J, McGuffey Jenna C, Di Venanzio G, Ortiz-Marquez Juan C, Weber Brent S, Lightly Tasia J, van Opijnen T, Scott Nichollas E, Cardona Silvia T, Feldman Mario F. 2022. The phenylacetic acid catabolic pathway regulates antibiotic and oxidative stress responses in *Acinetobacter*. *mBio* 13:e01863-21.

41. Teufel R, Mascaraque V, Ismail W, Voss M, Perera J, Eisenreich W, Haehnel W, Fuchs G. 2010. Bacterial phenylalanine and phenylacetate catabolic pathway revealed. *Proceedings of the National Academy of Sciences* 107:14390-14395.

42. Görke B, Stülke J. 2008. Carbon catabolite repression in bacteria: many ways to make the most out of nutrients. *Nature Reviews Microbiology* 6:613-624.

43. Ishige T, Tani A, Sakai Y, Kato N. 2000. Long-chain aldehyde dehydrogenase that participates in *n*-alkane utilization and wax ester synthesis in *Acinetobacter* sp. strain M-1. *Applied and Environmental Microbiology* 66:3481-3486.

44. Park C, Shin B, Park W. 2019. Alternative fate of glyoxylate during acetate and hexadecane metabolism in *Acinetobacter oleivorans* DR1. *Scientific Reports* 9:14402.

45. Morris FC, Jiang Y, Fu Y, Kostoulias X, Murray GL, Yu Y, Peleg AY. 2024. Lactate metabolism promotes in vivo fitness during *Acinetobacter baumannii* infection. *FEMS Microbiology Letters* 371:fnae032.

46. Sauer U, Eikmanns BJ. 2005. The PEP—pyruvate—oxaloacetate node as the switch point for carbon flux distribution in bacteria: We dedicate this paper to Rudolf K. Thauer, Director of the Max-Planck-Institute for Terrestrial Microbiology in Marburg, Germany, on the occasion of his 65th birthday. *FEMS Microbiology Reviews* 29:765-794.

47. Liu J, Wang D, Tong R, Ye S, Zhao Y, Wu J, Gan Y. 2025. Engineered rhizobia with trehalose-producing genes enhance peanut growth under salinity stress. *Agronomy* 15(4):974.

48. Zeidler S, Hubloher J, Schabacker K, Lamosa P, Santos H, Müller V. 2017. Trehalose, a temperature- and salt-induced solute with implications in pathobiology of *Acinetobacter baumannii*. *Environmental Microbiology* 19:5088-5099.

49. Mateo-Estrada V, Graña-Miraglia L, López-Leal G, Castillo-Ramírez S. 2019. Phylogenomics reveals clear cases of misclassification and genus-wide phylogenetic markers for *Acinetobacter*. *Genome Biology and Evolution* 11:2531-2541.

608 50. Vijayakumar S, Indranil B, and Veeraraghavan B. 2019. Accurate identification of clinically
609 important *Acinetobacter* Spp.: An update. *Future Science OA* 5:FSO395.

610 51. Durot M, Le Fèvre F, de Berardinis V, Kreimeyer A, Vallenet D, Combe C, Smidtas S,
611 Salanoubat M, Weissenbach J, Schachter V. 2008. Iterative reconstruction of a global metabolic
612 model of *Acinetobacter baylyi* ADP1 using high-throughput growth phenotype and gene
613 essentiality data. *BMC Systems Biology* 2:85.

614 52. Nogales J, García JL, Díaz E. 2017. Degradation of aromatic compounds in *Pseudomonas*: a
615 systems biology view, p 1-49. *In* Rojo F (ed), *Aerobic Utilization of Hydrocarbons, Oils and*
616 *Lipids*. Springer, Cham.

617 53. Park C, Shin B, Jung J, Lee Y, Park W. 2017. Metabolic and stress responses of *Acinetobacter*
618 *oleivorans* DR1 during long-chain alkane degradation. *Microbial Biotechnology* 10:1809-1823.

619 54. van Beilen Jan B, Funhoff Enrico G, van Loon A, Just A, Kaysser L, Bouza M, Holtackers R,
620 Röthlisberger M, Li Z, Witholt B. 2006. Cytochrome P450 alkane hydroxylases of the CYP153
621 family are common in alkane-degrading eubacteria lacking integral membrane alkane
622 hydroxylases. *Applied and Environmental Microbiology* 72:59-65.

623 55. Shingler V. 2003. Integrated regulation in response to aromatic compounds: from signal sensing
624 to attractive behaviour. *Environmental Microbiology* 5:1226-1241.

625 56. Lacal J, Busch A, Guazzaroni M-E, Krell T, Ramos JL. 2006. The TodS–TodT two-component
626 regulatory system recognizes a wide range of effectors and works with DNA-bending proteins.
627 *Proceedings of the National Academy of Sciences* 103:8191-8196.

628 57. Busch A, Guazzaroni M-E, Lacal J, Ramos JL, Krell T. 2009. The sensor kinase TodS operates
629 by a multiple step phosphorelay mechanism involving two autokinase domains. *Journal of*
630 *Biological Chemistry* 284:10353-10360.

631 58. Höring P, Rothschild-Mancinelli K, Sharma ND, Boyd DR, Allen CCR. 2016. Oxidative
632 biotransformations of phenol substrates catalysed by toluene dioxygenase: A molecular docking
633 study. *Journal of Molecular Catalysis B: Enzymatic* 134:396-406.

634 59. Spain JC, Zylstra GJ, Blake CK, Gibson DT. 1989. Monohydroxylation of phenol and 2,5-
635 dichlorophenol by toluene dioxygenase in *Pseudomonas putida* F1. *Applied and Environmental*
636 *Microbiology* 55:2648-2652.

637 60. Silva-Rocha R, de Lorenzo V. 2012. A GFP-*lacZ* bicistronic reporter system for promoter
638 analysis in environmental gram-negative bacteria. *PLOS ONE* 7:e34675.

639 61. Cosper Nathaniel J, Collier Lauren S, Clark Todd J, Scott Robert A, Neidle Ellen L. 2000.
640 Mutations in *catB*, the gene encoding muconate cycloisomerase, activate transcription of the
641 distalben genes and contribute to a complex regulatory circuit in *Acinetobacter* sp. strain ADP1.
642 *Journal of Bacteriology* 182:7044-7052.

643 62. Bundy BM, Collier LS, Hoover TR, Neidle EL. 2002. Synergistic transcriptional activation by
644 one regulatory protein in response to two metabolites. *Proceedings of the National Academy of*
645 *Sciences* 99:7693-7698.

646 63. Jiménez JI, Pérez-Pantoja D, Chavarría M, Díaz E, de Lorenzo V. 2014. A second chromosomal
647 copy of the *catA* gene endows *Pseudomonas putida* mt-2 with an enzymatic safety valve for
648 excess of catechol. *Environmental Microbiology* 16:1767-1778.

649 64. Werner AZ, Cordell WT, Lahive CW, Klein BC, Singer CA, Tan ECD, Ingraham MA, Ramirez
650 KJ, Kim DH, Pedersen JN, Johnson CW, Pfleger BF, Beckham GT, Salvachúa D. 2023. Lignin
651 conversion to β-ketoadipic acid by *Pseudomonas putida* via metabolic engineering and
652 bioprocess development. *Science Advances* 9:eadj0053.

653 65. Sazykin I, Sazykina M, Khmelevtsova L, Khammami M, Karchava S, Zhuravleva M,
654 Kudeevskaya E. 2016. Expression of SOD and production of reactive oxygen species in
655 *Acinetobacter calcoaceticus* caused by hydrocarbon oxidation. *Annals of Microbiology* 66:1039-
656 1045.

657 66. Rodríguez-Castro L, Durán RE, Méndez V, Dorochesi F, Zühlke D, Riedel K, Seeger M. 2024.
658 The long-chain flavodoxin FldX1 improves the biodegradation of 4-hydroxyphenylacetate and
659 3-hydroxyphenylacetate and counteracts the oxidative stress associated to aromatic catabolism in
660 *Paraburkholderia xenovorans*. *Biological Research* 57:12.

661 67. Cunningham L, Gruer MJ, Guest JR. 1997. Transcriptional regulation of the aconitase genes
662 (*acnA* and *acnB*) of *Escherichia coli*. *Microbiology* 143:3795-3805.

663 68. Jordan P, Tang Y, Bradbury AJ, Thomson AJ, JR. G. 1999. Biochemical and spectroscopic
664 characterization of *Escherichia coli* aconitases (AcnA and AcnB). *The Biochemical journal*
665 344:739-746.

666 69. Taboada B, Estrada K, Ciria R, Merino E. 2018. Operon-mapper: a web server for precise operon
667 identification in bacterial and archaeal genomes. *Bioinformatics* 34:4118-4120.

668 70. McClure R, Balasubramanian D, Sun Y, Bobrovskyy M, Sumby P, Genco CA, Vanderpool CK,
669 Tjaden B. 2013. Computational analysis of bacterial RNA-Seq data. *Nucleic Acids Research*
670 41:e140-e140.

673 **FIGURE LEGENDS**

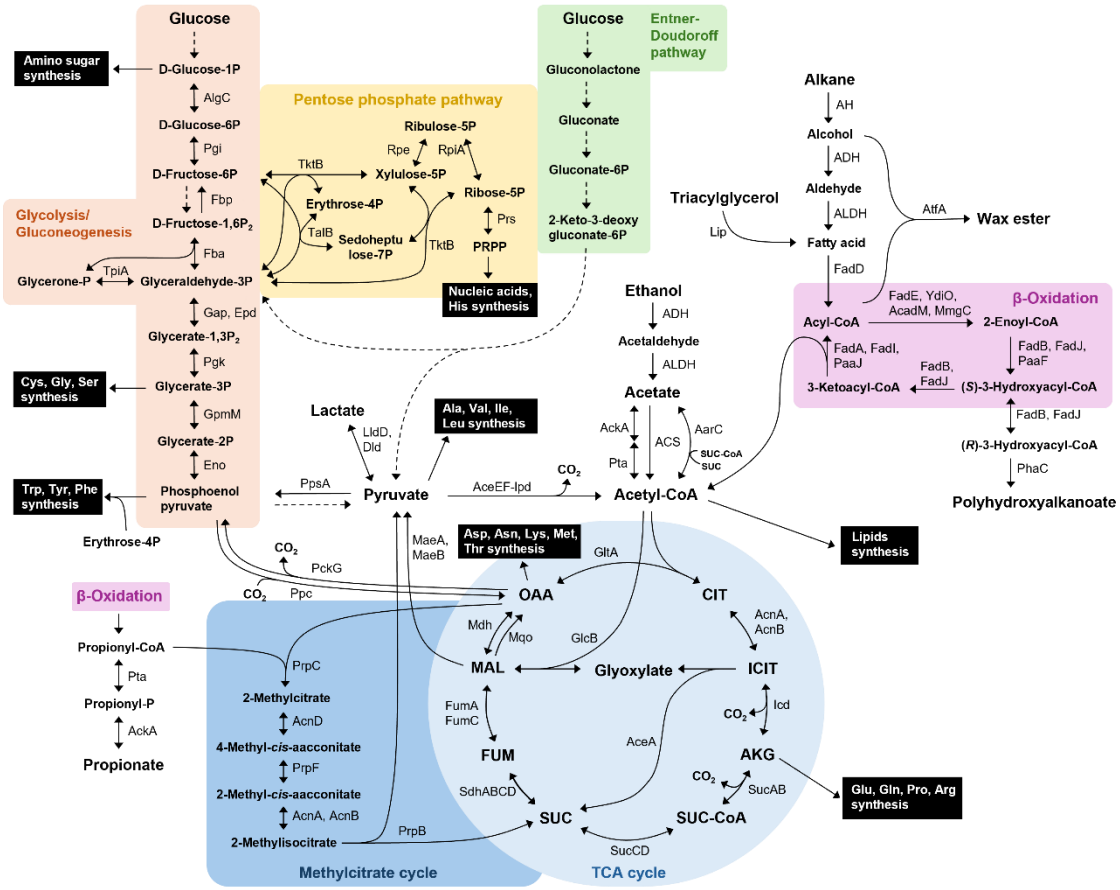

674

675 **Fig. 1.** Prediction of the central metabolic pathway of *Acinetobacter* sp. Tol 5. Genes related to the
676 central metabolic pathway were analyzed and listed in Table S2. Dashed arrows indicate metabolic
677 reactions for which the corresponding genes are not found in Tol 5 genome. Abbreviations: CIT;
678 citrate, ICIT; isocitrate, AKG; α-ketoglutarate, SUC-CoA; succinyl-CoA, SUC; succinate, FUM;
679 fumarate, MAL; malate, OAA; oxaloacetate, PRPP; phosphoribosyl pyrophosphate, AH; alkane
680 hydroxylase, ADH; alcohol dehydrogenase, ALDH; aldehyde dehydrogenase.

681

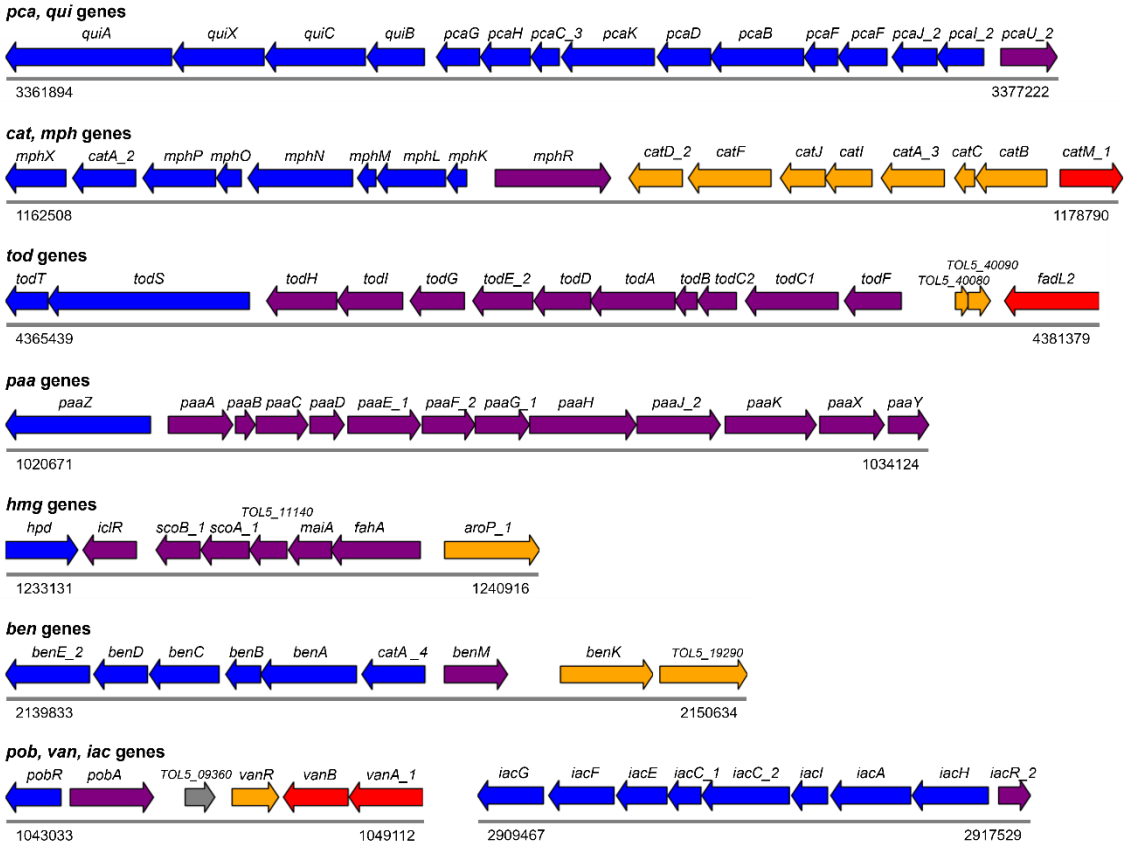

Fig. 2. Genetic organization of genes involved in the degradation of aromatic compounds in *Acinetobacter* sp. Tol 5. Predicted operon structures are illustrated based on analyses using Operon-mapper and Rockhopper. Genes within the same operon are represented by arrows of the same color. Proposed gene names or predicted functions are labeled above each arrow, and genomic coordinates are indicated below.

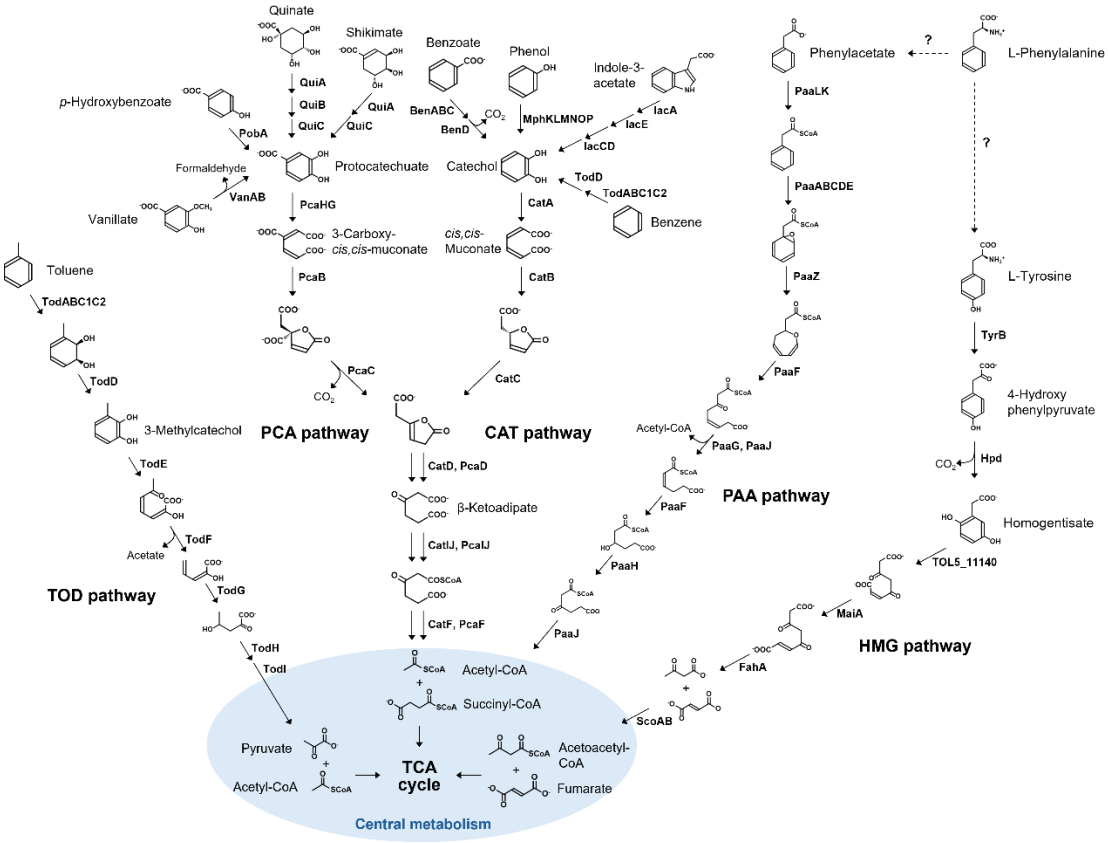

Fig. 3. Predicted degradation pathways of aromatic compounds in *Acinetobacter* sp. Tol 5, reconstructed based on the genes shown in Fig. 2 and Table S2. Question marks and dashed arrows indicate steps for which the genes encoding the corresponding enzymes have not been identified in Tol 5.

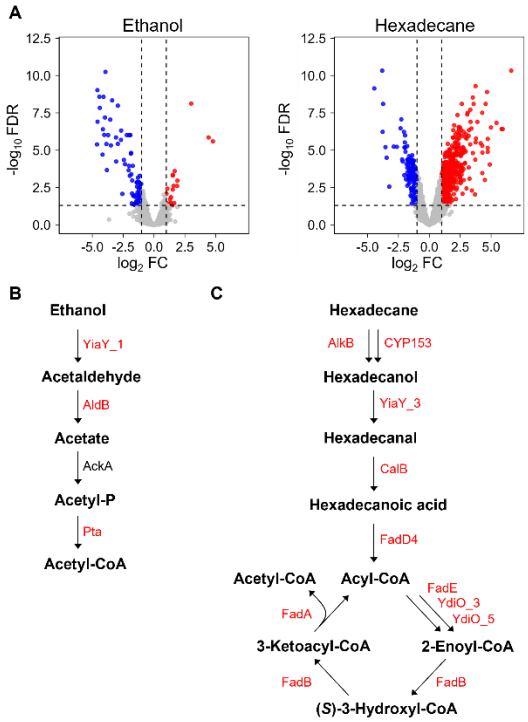

Fig. 4. Transcriptome analysis of *Acinetobacter* sp. Tol 5 grown on lactate, ethanol, and hexadecane. (**A**) Volcano plots comparing gene expression between lactate and ethanol (left) or hexadecane (right) as sole carbon sources (n = 3 biologically independent samples). Red and blue dots represent significantly upregulated and downregulated genes, respectively (FDR < 0.05, $|\log_2 FC| > 1$). (**B**, **C**) Proposed ethanol (**B**) and hexadecane (**C**) degradation pathways in Tol 5 based on transcriptome analysis. Genes encoding enzymes significantly upregulated under each condition are shown in red.

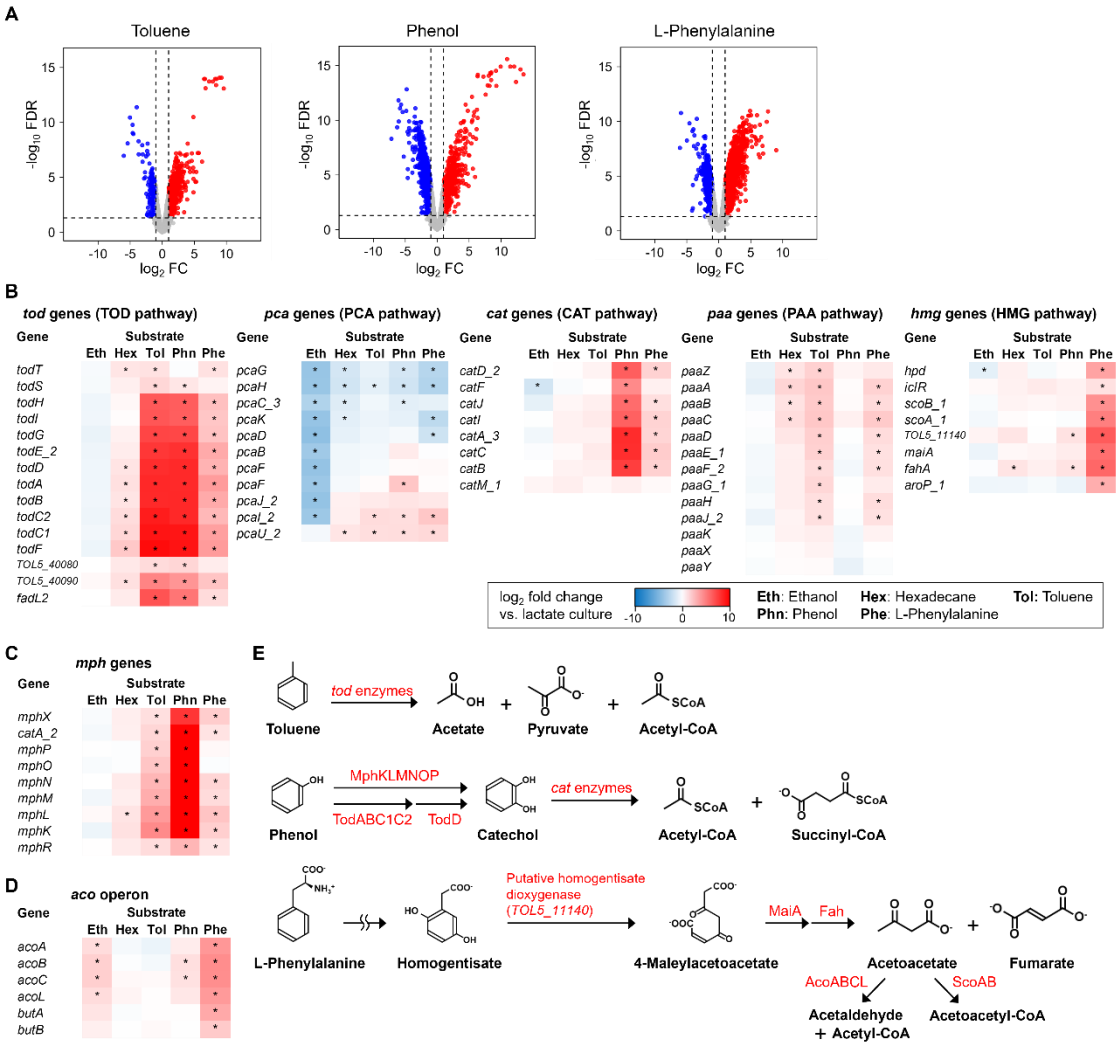

Fig. 5. Differential gene expression of *Acinetobacter sp.* Tol 5 grown on various aromatics, ethanol, and hexadecane, using lactate as the reference condition. (**A**) Volcano plots comparing gene expression between lactate and toluene (left), phenol (center), or L-phenylalanine (right) as sole carbon sources (n = 3 biologically independent samples). Red and blue dots represent significantly upregulated and downregulated genes, respectively (FDR < 0.05, $|\log_2 FC| > 1$). (**B-C**) Heat maps showing the average $\log_2$ FC of the genes involved in the five major aromatic degradation pathways (*tod*, *pca*, *cat*, *paa*, and *hmg* genes) (**B**), the *mph* genes (**C**), and the *aco* operon (**D**). The color gradient indicates the magnitude of the $\log_2$ FC values, with the deepest red representing ≥ 10 and the deepest blue representing ≤ -10. Asterisks (*) denote differentially expressed genes defined by $|\log_2 FC| > 1$, $\log_2$ CPM > 3, and FDR < 0.05. (**E**) Proposed aromatic substrates degradation pathways in Tol 5 based on transcriptome data. Genes encoding enzymes significantly upregulated under each condition are shown in red.

716

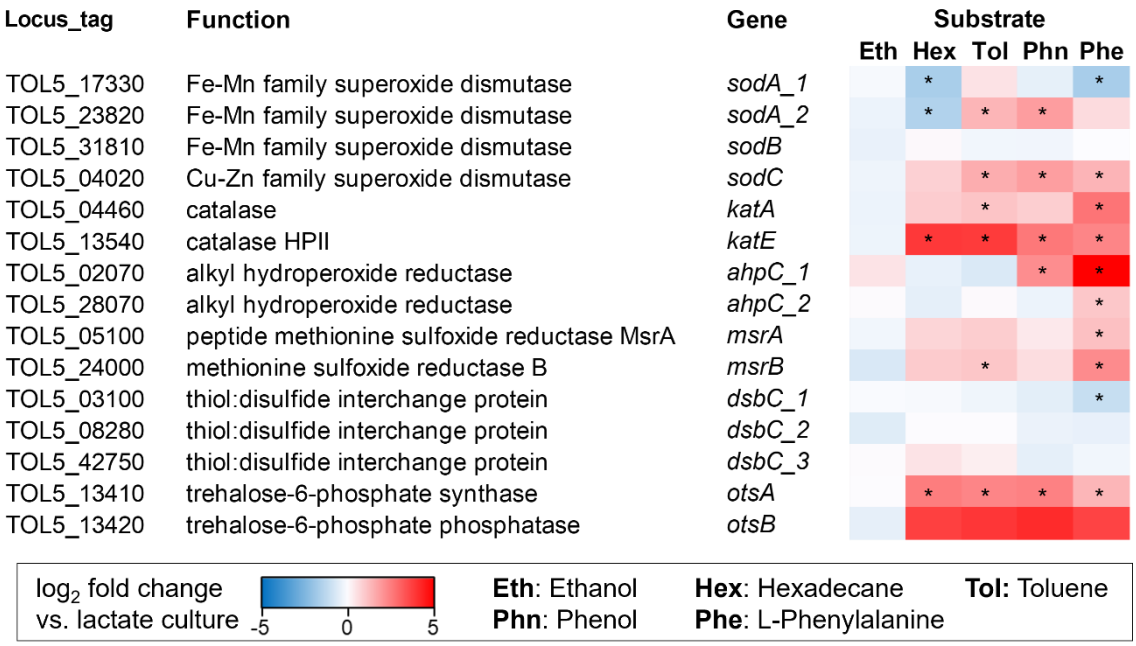

717

718 **Fig. 6.** Heat map showing the average $\log_2$ FC of genes involved in oxidative stress and osmotic
719 stress resistance. The color gradient indicates the magnitude of the $\log_2$ FC values, with the deepest
720 red representing ≥ 5 and the deepest blue representing ≤ -5. Asterisks (*) denote differentially
721 expressed genes defined by $|\log_2 \text{FC}| > 1$, $\log_2 \text{CPM} > 3$, and FDR < 0.05.

722